Extended Theory of Early-Late Code Tracking for a Bandlimited GPS Receiver

JOHN W. BETZ and KEVIN R. KOLODZIEJSKI
The MITRE Corporation, Bedford, Massachusetts

Received September 1999; Revised May 2000

ABSTRACT: *Code-tracking accuracy, an important attribute of GPS receivers, depends both on characteristics of the signal being tracked and on the design of the receiver. A simple expression has been available to predict code-tracking accuracy for early-late processing of signals with sinc-squared spectra in white noise for an infinite front-end bandwidth receiver. However, the literature has not indicated when this approximation holds. This paper provides a more exact analysis of code-tracking accuracy for early-late discriminators processing conventional binary phase shift keyed signals in white noise. New analytical expressions apply for various front-end bandwidths, discriminator spacings, and code-tracking loop bandwidths, while using linear models based on a small-error assumption. A theoretical lower bound is also supplied, indicating inherent limits on accuracy for given conditions. While evaluation of the exact expressions requires numerical integrations, new algebraic approximations are also provided. Numerical results compare the various expressions and approximations.*

INTRODUCTION

Theory has long been available for predicting the code-tracking accuracy of conventional biphase signals with pseudonoise spreading of rectangular chips for code-tracking loops using early-late discriminators and receivers having infinite front-end bandwidth. However, since all receiver front ends are bandlimited, it is necessary to know the conditions under which the infinite bandwidth approximation applies, and to characterize code-tracking errors when this approximation does not hold. Reference [1] presents this theory in the context of GPS, providing an algebraic approximation for infinite front-end bandwidth and outlining an approach for numerical calculations when the front-end bandwidth is finite.

Although the algebraic approximation in [1] has been applied to cases in which the front-end bandwidth is finite, later work has attempted to develop explicit theory that accounts for bandlimiting at the receiver front end [2]. This extension does not completely avoid assumptions of infinite bandwidth, and thus yields misleading results. In particular, it does not account for the effects of noise correlation due to front-end bandlimiting.

NAVIGATION: *Journal of The Institute of Navigation*
Vol. 47, No. 3, Fall 2000
Printed in the U.S.A.

The code-tracking performance of a receiver with a bandlimited front end is of increasing importance. Advances in receiver technology enable wider bandwidths and narrower early-late spacing. The emerging question is what values are best, rather than what values can be built. Very wide-bandwidth C/A-code receivers with narrow early-late spacing are being built; while the primary motivation is discrimination against multipath, it is important to understand the consequences for code-tracking accuracy in white noise. In addition, the new civil signal design at L5 (1176.45 MHz) employs 10.23 MHz chip rates [3]; the infinite bandwidth theory does not fully apply for this important situation.

This paper presents new expressions that (as long as the standard assumptions apply) accurately describe code-tracking accuracy in white noise with any degree of bandlimiting, along with a new closed-form approximation and the conditions under which this approximation applies. All of the discussion in this paper assumes that the early-late spacing in the discriminator is less than or equal to a chip period, and that the receiver front-end bandwidth is wide enough to pass at least half the main lobe of the signal's sinc-squared spectrum. We show that the infinite bandwidth approximation [1] applies when the receiver is spacing-limited: when the product of the front-end complex bandwidth (in hertz) and the (two-sided) early-late spacing (in seconds) is greater than π. As has been shown [1], the approximate normalized code-tracking error in the spacing-limited case depends on the early-late spacing, and not the receiver front-end bandwidth.

The infinite bandwidth approximation does not hold, and a new approximation is supplied, when the receiver is bandwidth-limited: the product of the front-end complex bandwidth (in hertz) and the (two-sided) early-late spacing (in seconds) is less than unity. In the bandwidth-limited case, the approximate normalized code-tracking error depends on the receiver front-end bandwidth, and not the early-late spacing. The previous expression [2] is not accurate for the bandwidth-limited case. A new approximation is also supplied for the transition region between the spacing-limited case and the bandwidth-limited case.

A qualitative description of the problem being analyzed and an intuitive explanation of the results help motivate the remainder of this paper. It has been established that analysis of code-tracking accuracy, under conventional assumptions of stationary noise, no dynamics, and moderate or high signal-to-noise ratio, can proceed by modeling a noncoherent early-late code-tracking loop in linearized form: the difference in estimated power between early and late correlator taps provides an error signal, which is scaled by the discriminator gain and smoothed in the code-tracking loop.

Bandlimiting of the signal smoothes its correlation function, tending to reduce the discriminator gain and increase code-tracking error. This effect has been accounted for in previous attempts to analyze the effects of limited front-end bandwidth. But a further effect occurs that has not previously been taken into account: bandlimiting of the noise introduces additional correlation between the error at the early tap and the error at the late tap, beyond the correlation introduced at smaller chip spacings from correlating the noise against the early and late reference signals. The consequence is that the code-tracking error of bandlimited receivers can differ from what has been predicted previously.

One consequence of this new and more accurate theory involves application of the discriminator gain. While it has long been recognized that larger discriminator gain implies improved code-tracking accuracy for infinite bandwidth receivers, this relationship does not necessarily hold except in the spacing-limited case. If the front-end bandwidth is not extremely large, there is a point of diminishing returns in the reduction of code-tracking error once the early-late spacing becomes smaller than the reciprocal of the receiver bandwidth, even though the discriminator gain may continue to increase.

Furthermore, over relatively small ranges of front-end bandwidths and early-late spacings, the root-mean-squared (RMS) code-tracking error oscillates over a peak-to-peak range more than 25 percent. Choosing appropriately matched bandwidth and spacing can significantly lower the noise-related contribution to code-tracking error.

Finally, we also show that, for any fixed front-end bandwidth and high enough signal power, the code-tracking error converges, for vanishing early-late spacing, to a lower bound (LB) computed for the bandlimited signal. This result is in contrast to previous claims [2].

This paper draws on a more general theory of code-tracking accuracy developed in [4, 5]. While the more general theory applies to signals with arbitrary spectra and for additive Gaussian noise having arbitrary spectra, this paper focuses on the case of bandlimited white noise and signals having sinc-squared spectra, such as the conventional signals used for C/A-code and P(Y)-code and the new civil signal proposed for L5. In contrast with the more detailed development in [4, 5], this paper emphasizes results and their application and interpretation.

The following analysis applies to conditions that satisfy a set of fundamental assumptions. It is assumed that the integration time used in the discriminator is long—much longer than the reciprocal of the receiver front-end bandwidth. The signal is assumed to be a known (to the receiver) segment of pseudorandomly modulated direct sequence spread-spectrum chips. Any effects from short periods of the spreading code (e.g., for C/A-code [6]) are deemed to be negligible in white noise. The noise is statistically stationary, white, and Gaussian. The resulting errors are assumed to be small, so that the linearized analysis applies.

The paper models the code-tracking loop as an estimator of the time of arrival (TOA) of the received signal. The next section defines the problem being analyzed, introduces the notation and assumptions that are employed, and shows how the tracking loop affects errors from TOA estimation. The following section presents exact analytical results (within the conventional assumptions used) that predict code-tracking accuracy in bandlimited white noise, derives new approximations to these exact expressions, and compares the new approximations and previous expressions. This section also presents a lower bound on code-tracking accuracy that applies for any discriminator with a bandlimited receiver. A set of numerical results is then presented to explore and compare the different expressions and approximations. The last section summarizes the results and discusses their implications.

PROBLEM FORMULATION AND MATHEMATICAL MODELS

This section formulates the problem being analyzed, introducing notation and describing the overall processing flow under consideration. It provides mathematical models and assumptions, and defines some common quantities that are employed in subsequent sections.

The analysis uses complex baseband representations of signals and noise, and lowpass equivalent models of filtering and processing. Thus, frequency values of zero in the baseband representations correspond to the carrier frequency of the radio frequency signal.

Assume a (complex-valued) signal $s(t)$ that is known (except for unknown delay and carrier phase) at the receiver. It is assumed that the frequency of arrival is known perfectly. However, as long as the frequency of arrival is known to within a fraction of the reciprocal of the coherent integration time, this approximation is valid. The received data is then the sum of the signal and white noise, $n(t)$. The received data is observed over a long time interval T_{obs}: $x(t) = e^{i\theta}s(t - t_0) + n(t),\ 0 \le t \le T_{obs}$, where the unknown delay, or time of arrival, t_0, is defined relative to an arbitrary origin, and θ is the carrier phase. Consistent with most analyses of code-tracking accuracy, it is assumed that t_0 either is fixed or has time variation that is being tracked perfectly by the receiver over the time period of interest, so no dynamics need be considered explicitly. However, the results hold as long as any change in t_0 not tracked by the receiver is somewhat slower than the reciprocal bandwidth of the code-tracking loop.

The integration time in the discriminator is denoted T, while the (one-sided) equivalent rectangular bandwidth (also known as the noise equivalent bandwidth) of the code-tracking loop is denoted B_L. Furthermore, it is assumed that T_{obs} is much greater than $1/B_L$, and that the analysis is not concerned with the transient start-up phase, so the time frame of interest is $1/B_L \ll t \le T_{obs}$.

Since the signal is modeled as known and not a random process at the receiver, a power spectral density is found as follows. The Fourier transform of the signal observed over the time interval $(k-1)T \le t < kT$ is denoted $S_{kT}(f)$:

$$S_{kT}(f) = \int_{(k-1)T}^{kT} s(t - t_0)e^{-i2\pi ft}\,dt \qquad (1)$$

Define a power spectral density as $|S_{kT}(f)|^2/T$, and recognize that, as long as T includes many chip periods, $|S_{kT}(f)|^2/T$ is approximately the same for any value of k. The signal's power spectral density is then denoted by $C_sG_s(f) = |S_{kT}(f)|^2/T$, where $G_s(f)$ is defined as a power spectral density normalized to unit power over infinite bandwidth

$$\int_{-\infty}^{\infty} G_s(f)\,df = 1 \qquad (2)$$

and C_s is commonly referred to as the signal carrier power, also defined over an infinite bandwidth. It is assumed that this power spectral density is symmetric about $f = 0$. The noise is white with power spectral density N_0, so that the signal has a carrier power-to-noise density ratio of C_s/N_0 Hz.

Signals of interest here are phase shift keyed (PSK) signals with rectangular chip shapes (i.e., non-return-to-zero chips). For conciseness, we refer to these modulations in this paper as conventional PSK signals, in contrast, for example, with the subcarrier signals described in [7]. For the conventional PSK signals, if the chip period is T_c, the normalized power spectrum of the signal is

$$G_s(f) = T_c\,\mathrm{sinc}^2(\pi f T_c) \qquad (3)$$

where we neglect any spectral lines introduced by short spreading codes.

It is well known (see equation (B-8)) in [8], for example) that when the receiver front end has complex bandwidth β_r (produced with "ideal filtering" —a rectangular bandpass filter with no phase response), correlation of the received signal plus noise with the reference signal produces a maximum output signal-to-noise ratio (SNR)

$$\rho_o \cong \frac{TC_s}{N_0}\int_{-\beta_r/2}^{\beta_r/2} G_s(f)\,df = \frac{TC_s}{N_0}\int_{-b/2}^{b/2} \mathrm{sinc}^2(\pi f)\,df \qquad (4)$$

where the approximation applies for output SNR somewhat greater than unity, the normalized receiver front-end bandwidth is denoted $b = T_c\beta_r$, and the integral indicates the fraction of signal power passed by the receiver front end.

This paper evaluates different code-tracking loop approaches that all satisfy the canonical form illustrated in Figure 1. The received signal plus noise enters a discriminator, which effectively is an estimator of the signal's TOA. A previous estimate of

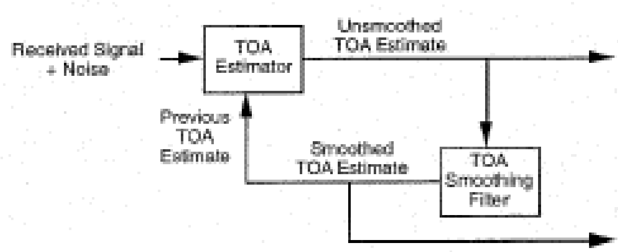

Fig. 1 – Representation of Code-Tracking Loop

the signal's TOA is also provided to this TOA estimator, which uses an integration time of T seconds to produce an unsmoothed TOA estimate. This estimate is the update to the previous TOA estimate based on the received signal plus noise. Unsmoothed TOA estimates are processed by a TOA smoothing filter, producing smoothed estimates that are provided to the TOA estimator as previous estimates.

Different versions of the TOA estimator are considered in this analysis. When the TOA is estimated from early-late processing of the cross-correlation between the received signal plus noise and a reference signal, noncoherent early-late processing (NELP) involves the magnitude-squared of this cross-correlation, implying no knowledge of alignment between the phase of the reference signal and that of the received signal. Coherent early-late processing (CELP) uses only the in-phase part of the cross-correlation function, implying perfect alignment between the phase of the reference signal and that of the reference signal. Finally, an LB on code-tracking error is obtained based on the Cramér-Rao lower bound on TOA estimation, given the integration time used in the TOA estimator.

Although the code-tracking loop representation in Figure 1 differs from those traditionally shown (in [9], for example), it is mathematically equivalent under the conventional linearizing assumptions used to analyze code-tracking error. This representation was selected to show explicitly the distinction and the relationship between the TOA estimator and the TOA smoothing filter. Of course, the smoothed TOA estimate is the conventional output of the code-tracking loop—the current estimate of the timing of the received code.

As described in [4, 5], the TOA estimator in Figure 1 is modeled as performing block processing, processing the received signal plus noise over each T seconds, and using the smoothed TOA estimate τ_k^s as the previous TOA estimate to provide an unsmoothed TOA estimate that persists for the subsequent T seconds until it is replaced by the next unsmoothed TOA estimate. The unsmoothed TOA estimate produced at kT seconds is denoted τ_k^u. Consistent with most analyses of code-tracking accuracy, it is assumed that the unsmoothed TOA estimates are unbiased and that the errors are small. Hence, the conditional mean of τ_k^u is $E\{\tau_k^u \mid \tau_k^s\} = t_0$, and its variance is $Var\{\tau_k^u \mid \tau_k^s\} = E\{(\tau_k^u - t_0)^2 \mid \tau_k^2\} = \sigma_u^2$.

It is shown in [4, 5] that for $0 < TB_L < 0.5$, the variance of the code-tracking loop output is approximately related to the variance of the unsmoothed TOA estimate by

$$\sigma_\tau^2 = Var\{\tau_k^s\} \cong \sigma_u^2 2B_L T(1 - 0.5B_L T) \qquad (5)$$

This relationship between the variance of unsmoothed TOA estimate and variance of smoothed TOA estimate is independent of the specific processing used to obtain the unsmoothed TOA estimate, as long as the estimation process conforms to the canonical form shown in Figure 1.

Observe that equation (5) implies that the code-tracking loop bandwidth is constant in the expression for variance of the code-tracking loop output. In practice, this may not be the case, since changing the early-late spacing changes the loop gain and hence the loop bandwidth (see [10], for example). Numerical calculations performed by the authors have shown that for limited front-end bandwidths, the discriminator gain diminishes as the early-late spacing becomes small, increasing the loop bandwidth and thus the output variance (equation (5)). Attempts using computer simulations or hardware to explore the behavior described in this paper must either account for this change in loop bandwidth or keep the loop gain (hence the loop bandwidth) constant as the early-late spacing is modified.

ANALYTICAL RESULTS

Early-late processing is one of the more common approaches used for TOA estimation in the code-tracking process portrayed in Figure 1, or equivalently as a discriminator. Noncoherent processing, which does not rely on knowledge or estimates of the carrier phase, is of interest, as well as coherent processing. The LB calculated for a bandlimited signal provides a bound on processing performance.

While analytical results for various discriminator processing approaches have been developed by the authors, this paper concentrates for simplicity on early-late processing, carrying along the LB for reference. General expressions for code-tracking accuracy using early-late processing are based on the derivations in [4]. While these expressions are exact under the assumptions given, they are complicated, do not provide much insight, and require numerical integrations in their evaluation. Exact expressions are presented for the special case of conventional PSK signals in bandlimited white noise, which are much simpler but still require numerical evaluation. We also present simpler approximations, derived from the exact expressions, that can be evaluated using algebra, as well as the conditions under which these approximations hold.

General expressions for code-tracking accuracy in white noise with a bandlimited receiver front end and early-late discriminator are obtained from those in the appendix, which are not restricted to white noise. The following results hold for conventional PSK signals with chip period T_c seconds in white noise when the integration time used to form a correlation estimate in the discriminator is T seconds (assumed to be much longer than T_c); the bandlimiting at the receiver is represented by a rectangular bandpass filter with complex bandwidth β_r Hz (assumed to be much larger than 1/T), $\beta_r = b/T_c$; B_L is the one-sided code-tracking loop bandwidth in hertz (assumed to be less than 0.5/T); $\Delta = DT_c$ is the (two-sided) early-late spacing in seconds; $G_s(f)$ is the normalized (unit area) power spectral density of the signal in 1/Hz; C_s is the signal carrier power over infinite bandwidth in watts; and N_0 is the power spectral density of white Gaussian noise in watts/hertz.

Figure 2 illustrates the definition of the normalized front-end complex bandwidth, b. Figure 3 illustrates the definition of the normalized two-sided discriminator spacing D.

An LB on code-tracking error variance, denoted σ_τ^2 in units of seconds squared, for a given front-end filter bandwidth and given code-tracking loop is obtained by substituting $G_w(f) = N_0$ into equation (14), yielding the normalized code-tracking error variance.

$$\left(\frac{\sigma_\tau^2}{T_c^2}\right)_{LB} = \frac{B_L(1-0.5B_LT)}{(2\pi)^2T_c^3\frac{C_s}{N_0}\int_{-\beta_r/2}^{\beta_r/2} f^2\,\mathrm{sinc}^2(\pi f T_c)\,df}$$
$$= \frac{B_L(1-0.5B_LT)}{2\beta_rT_c\frac{C_s}{N_0}[1-\mathrm{sinc}(\pi\beta_rT_c)]}$$
$$= \frac{B_L(1-0.5B_LT)}{2b\frac{C_s}{N_0}[1-\mathrm{sinc}(\pi b)]} \quad (6)$$

Using the observation that for $0 < b < 1$, $1 - \mathrm{sinc}(\pi b) \cong b$, while for $1 \le |b|$, $1 - \mathrm{sinc}(\pi b) \cong 1$, equation (6) can be approximated as

$$\left(\frac{\sigma_\tau^2}{T_c^2}\right)_{LB} \cong \begin{cases} \dfrac{B_L(1-0.5B_LT)}{2\frac{C_s}{N_0}b^2}, & b \le 1 \\[2ex] \dfrac{B_L(1-0.5B_LT)}{2\frac{C_s}{N_0}b}, & b > 1 \end{cases} \quad (7)$$

Note that the LB does not depend on the early-late spacing, but instead relates how well any discriminator can perform with a given front-end bandwidth.

Substituting $G_w(f) = N_0$ into equation (12) and performing some manipulations yields the error variance of a code-tracking loop using NELP, in normalized units of chip periods squared:

$$\left(\frac{\sigma_\tau^2}{T_c^2}\right)_{NELP} = \frac{B_L(1-0.5B_LT)\int_{-b/2}^{b/2}\mathrm{sinc}^2(\pi f)\sin^2(\pi fD)\,df}{(2\pi)^2\frac{C_s}{N_0}\left(\int_{-b/2}^{b/2} f\,\mathrm{sinc}^2(\pi f)\sin(\pi fD)\,df\right)^2} \times\left[1+\frac{\int_{-b/2}^{b/2}\mathrm{sinc}^2(\pi f)\cos^2(\pi fD)\,df}{T\left(\frac{C_s}{N_0}\right)\left(\int_{-b/2}^{b/2}\mathrm{sinc}^2(\pi f)\cos(\pi fD)\,df\right)^2}\right] \quad (8)$$

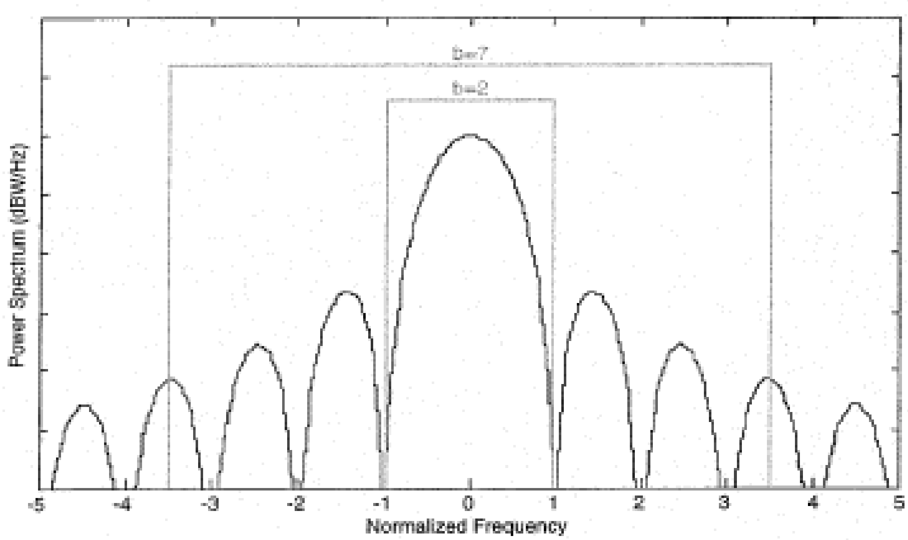

Fig. 2 – Signal Power Spectral Density and Two Different Values of Normalized Front-End Bandwidth (b)

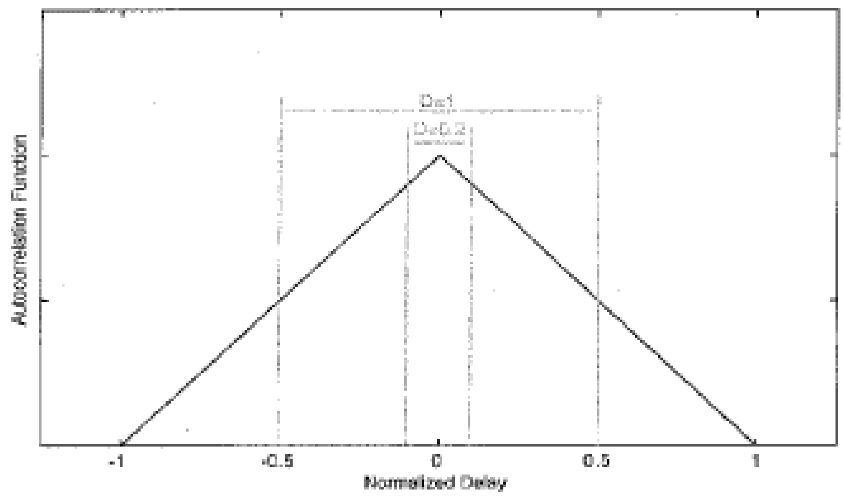

Fig. 3 – Ideal Signal Autocorrelation Function and Two Different Values of Normalized Early-Late Spacing (D)

Considerable manipulation of equation (8), using a variety of trigonometric identities and series approximations, yields approximations for three cases of particular interest under the constraint that $b > 1$, which is ensured when the front-end filter is wide enough to pass the center half of the signal spectrum's main lobe. The resulting approximation is

$$\left(\frac{\sigma_\tau^2}{T_c^2}\right)_{NELP} \cong \begin{cases} \dfrac{B_L(1-0.5B_LT)}{2\dfrac{C_s}{N_0}} D\left[1+\dfrac{2}{T\dfrac{C_s}{N_0}(2-D)}\right], & \pi \le Db \\ \dfrac{B_L(1-0.5B_LT)}{2\dfrac{C_s}{N_0}}\left[\dfrac{1}{b}+\dfrac{b}{\pi-1}\left(D-\dfrac{1}{b}\right)^2\right]\left[1+\dfrac{2}{T\dfrac{C_s}{N_0}(2-D)}\right], & 1 < Db < \pi \\ \dfrac{B_L(1-0.5B_LT)}{2\dfrac{C_s}{N_0}}\left(\dfrac{1}{b}\right)\left[1+\dfrac{1}{T\dfrac{C_s}{N_0}}\right], & Db \le 1 \end{cases} \tag{9}$$

The condition $\Delta\beta_r = Db \ge \pi$ is referred to as *spacing-limited*, since the error depends primarily on the early-late spacing and not the front-end bandwidth. The condition $\Delta\beta_r = Db < 1$ is referred to as *bandwidth-limited*, since the error depends primarily on the front-end bandwidth and not the early-late spacing. The condition $1 < Db < \pi$ indicates a transition region between the two distinct limiting cases. These three different regions are illustrated in Figure 4.

Given the above, it is straightforward to show [4] that for CELP, the error variance is

$$\left(\frac{\sigma_\tau^2}{T_c^2}\right)_{CELP} = \frac{B_L(1-0.5B_LT)\int_{-b/2}^{b/2}\operatorname{sinc}^2(\pi f)\sin^2(\pi f D)\,df}{(2\pi)^2\dfrac{C_s}{N_0}\left(\int_{-b/2}^{b/2} f\operatorname{sinc}^2(\pi f)\sin(\pi f D)\,df\right)^2} \tag{10}$$

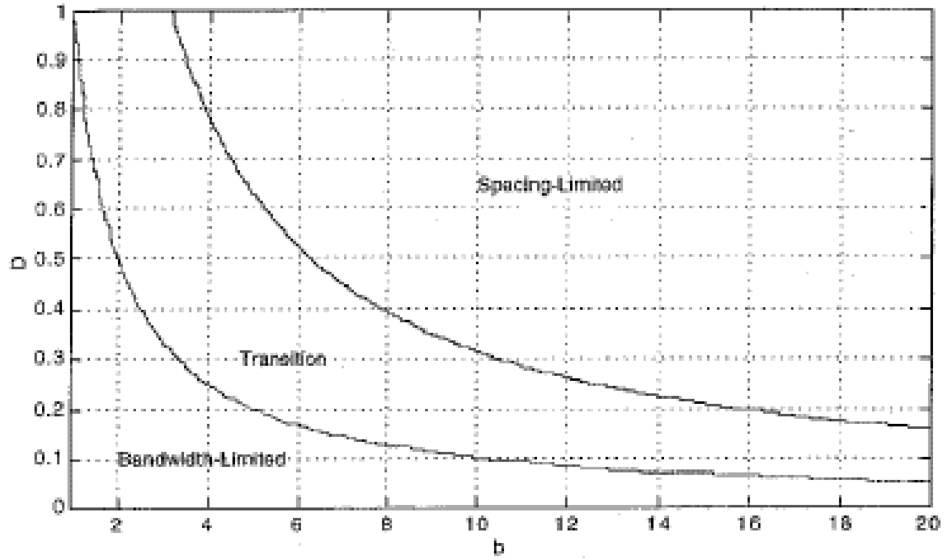

Fig. 4 – Region Boundaries in Discriminator Parameter Space Where Different Approximations Apply

which can be approximated, again using a variety of trigonometric identities and series approximations, as

$$\left(\frac{\sigma_\varepsilon^2}{T_c^2}\right)_{CELP} \cong \begin{cases} \dfrac{B_L(1-0.5B_LT)}{2\dfrac{C_s}{N_0}}D, & \pi \le Db \\[2ex] \dfrac{B_L(1-0.5B_LT)}{2\dfrac{C_s}{N_0}}\left[\dfrac{1}{b}+\dfrac{b}{\pi-1}\left(D-\dfrac{1}{b}\right)^2\right], & 1 < Db < \pi \\[2ex] \dfrac{B_L(1-0.5B_LT)}{2\dfrac{C_s}{N_0}}\left(\dfrac{1}{b}\right), & Db \le 1 \end{cases} \tag{11}$$

The result for coherent early-late processing is a lower bound on noncoherent early-late processing. The two diverge significantly only when the ideal postcorrelation SNR, TC_s/N_0, is small.

Note that while the code-tracking error, expressed in fractional chip periods, is independent of the chip period for the spacing-limited case when the front-end bandwidth is large, the error variance is inversely proportional to the normalized bandwidth and independent of the early-late spacing for the bandwidth-limited case. Also, the expression in equation (11) for the bandwidth-limited case is identical to the lower bound in equation (7), indicating that once the discriminator spacing is less than the reciprocal of the front-end bandwidth, early-late processing provides optimal performance, and that there is no benefit (in terms of code-tracking accuracy in white noise) to further reducing the early-late spacing.

NUMERICAL RESULTS FOR NONCOHERENT EARLY-LATE PROCESSING

The results in this section compare numerical calculations that use the expression for LB (equation (6)), the expression for noncoherent early-late processing with infinite bandwidth from [1], the previous expression for finite front-end bandwidths from [2], the exact expression for noncoherent early-late processing (equation (8)), and the new approximation for noncoherent early-late processing (equation (9)). The results are calculated using a coherent integration time of T = 0.02 s and a code-tracking loop bandwidth (one-sided equivalent rectangular bandwidth) of 1 Hz.

Figure 5 shows the normalized code-tracking error predicted by the exact expression of equation (8) over a range of normalized front-end bandwidths and discriminator spacings. The error tends to be smaller for larger bandwidths and smaller discriminator spacings, with an oscillatory structure superposed for larger values of b and D.

Figure 6 shows, in contrast, the normalized code-tracking error predicted using the infinite bandwidth approximation from [1], which is equivalent to using the expression for the spacing-limited ($Db \geq \pi$) case in equation (9) over all values of b and D. Unlike the exact expression in Figure 5, Figure 6 shows no dependence on front-end bandwidth, shows the error approaching zero for dimin-

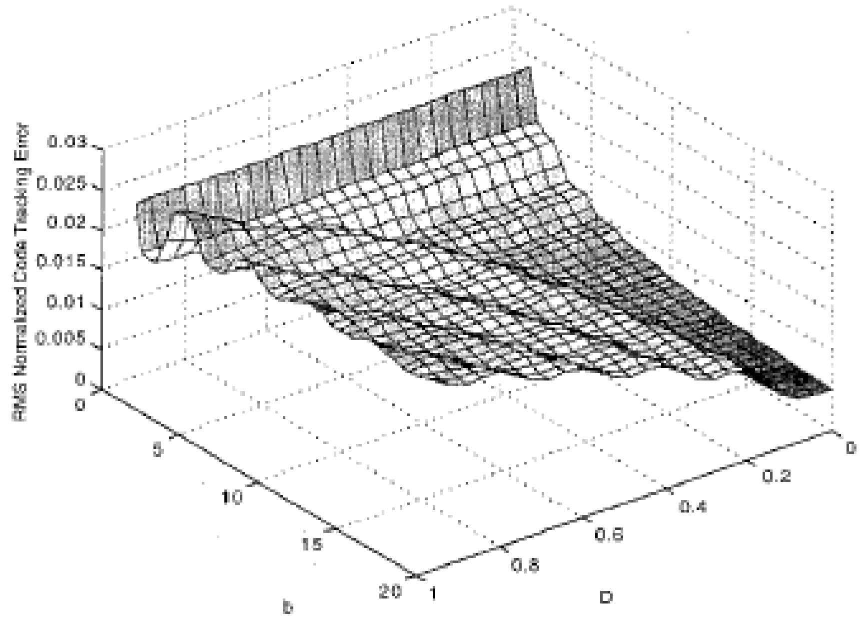

Fig. 5 - Exact Expression (equation (8)) Evaluated at C_s/N_0 of 30 dB-Hz

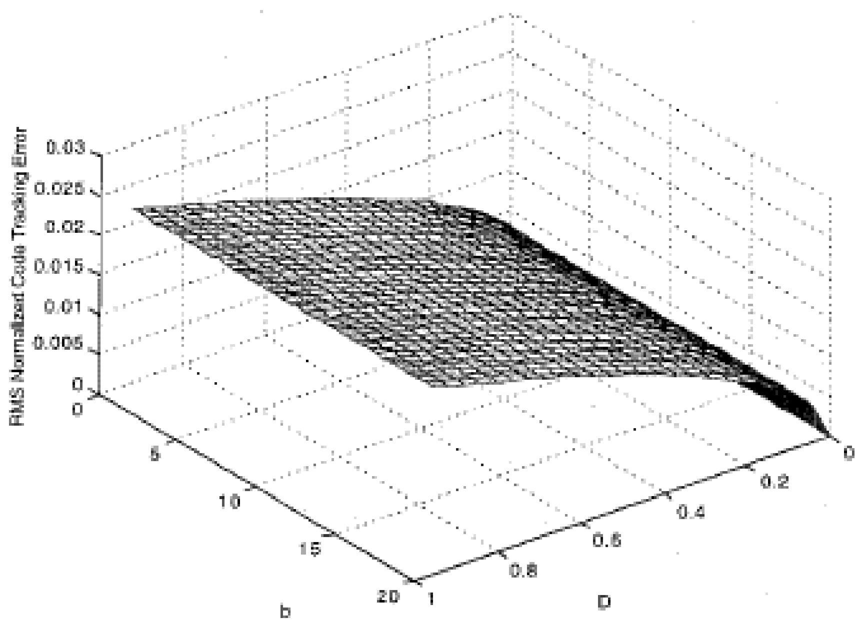

Fig. 6 - Infinite Bandwidth Approximation Evaluated at C_s/N_0 of 30 dB-Hz

ishing early-late spacing, and does not display any of the oscillatory structure.

Figure 7 shows the absolute value of the fractional error between the infinite bandwidth approximation shown in Figure 6 and the exact expression shown in Figure 5. While the error in the approximation is quite small for large bandwidth and large early-late spacing, it increases in an arc whose location in the D-b plane corresponds to the location of the transition region portrayed in Figure 4. The approximation error becomes very large for small values of D, corresponding to the bandwidth-limited case.

Figure 8 shows the normalized code-tracking error predicted using the previous expression from [2], which, like the exact expression shown in Figure 5, must be evaluated numerically. Like the exact expression in Figure 5, Figure 8 shows dependence on front-end bandwidth and displays some oscillatory structure. However, it predicts that the

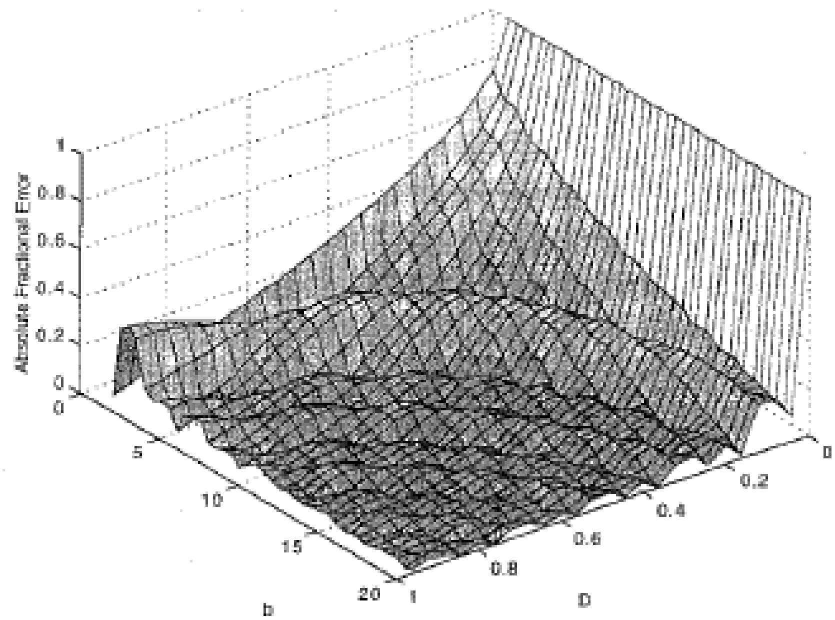

Fig. 7 – Absolute Value of Fractional Error Between Infinite Bandwidth Approximation and Exact Expression, with Larger Absolute Error Indicated by Lighter Shading

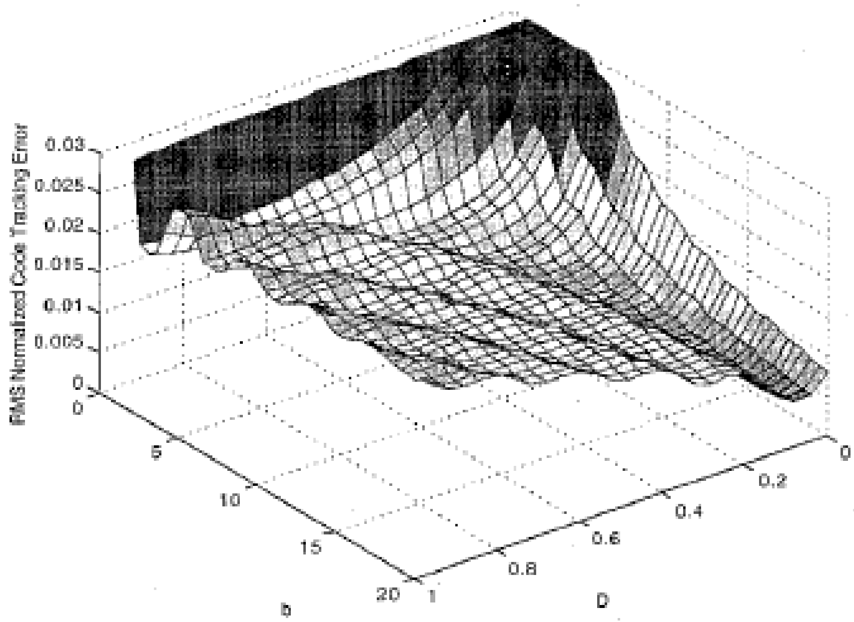

Fig. 8 – Previous Expression Evaluated at C_s/N_0 of 30 dB-Hz

error increases for small bandwidth or for small spacing, and the plot is truncated near the origin.

Figure 9 shows the absolute value of the fractional error between the previous expression shown in Figure 8 and the exact expression shown in Figure 5. While the error is quite small over much of the plane (note that it benefits from numerical integration rather than algebraic approximation), it increases in an arc whose location in the D-b plane corresponds roughly to the location of the bandwidth-limited region portrayed in Figure 4. The approximation error becomes very large for small values of D, corresponding to the bandwidth-limited case.

Figure 10 shows the normalized code-tracking error predicted using the new approximation (equation (9)). While the surface does not display the oscillatory structure in the exact expression (allow-

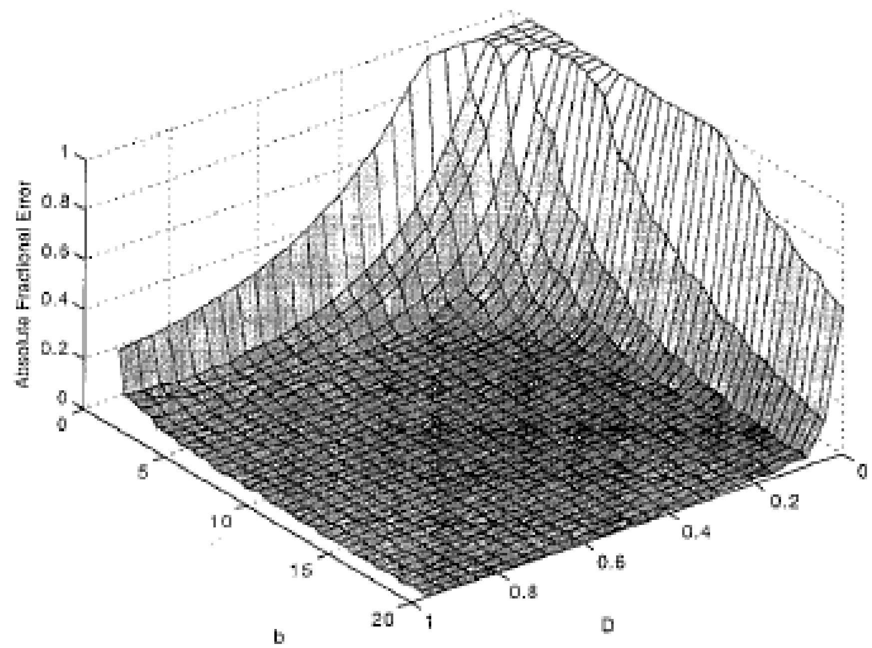

Fig. 9 – Absolute Value of Fractional Error Between Previous Expression and Exact Expression, with Larger Absolute Error Indicated by Lighter Shading

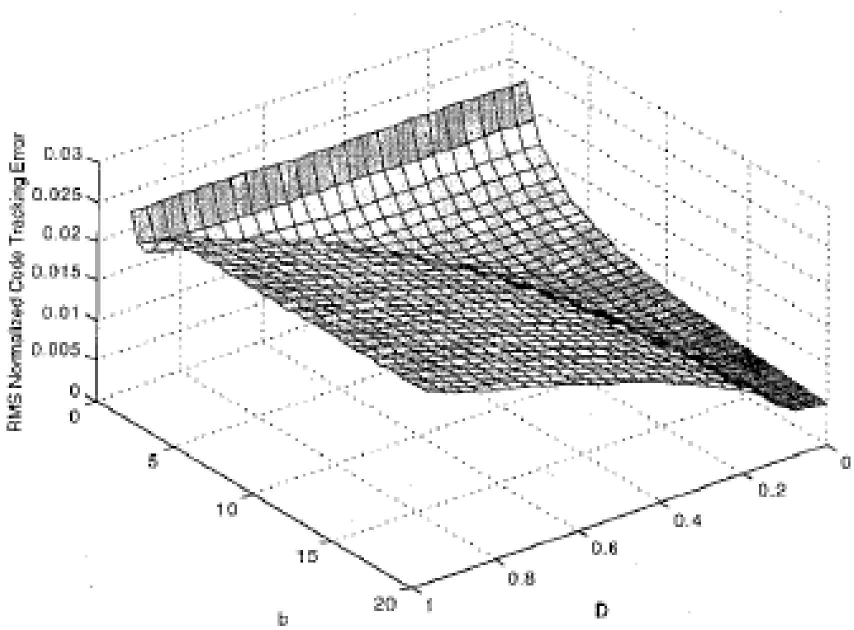

Fig. 10 – New Approximation Evaluated at C_s/N_0 of 30 dB-Hz

ing the algebraic expression to remain simple), it correctly shows the increased code-tracking error with diminished front-end bandwidth, and also shows that the error approaches a nonzero asymptote with diminishing early-late spacing.

Figure 11 shows the absolute value of the fractional error between the new approximation shown in Figure 10 and the exact expression shown in Figure 5. The error in the approximation is consistently small over the entire range of parameters—a substantial improvement over the previous expression for cases with small early-late spacing or front-end bandwidths that are not significantly larger than the chip rate.

While the surfaces shown in the preceding figures indicate qualitatively the behavior of the exact expression and the approximations, more quantitative results are obtained by considering slices of these surfaces. Figure 12 shows predicted code-tracking error for C_s/N_0 of 30 dB-Hz and normalized front-end bandwidth of b = 10—a wide front-end bandwidth. Except for the oscillatory behavior predicted by the exact expression, the infinite bandwidth approximation is accurate for wider discrimi-

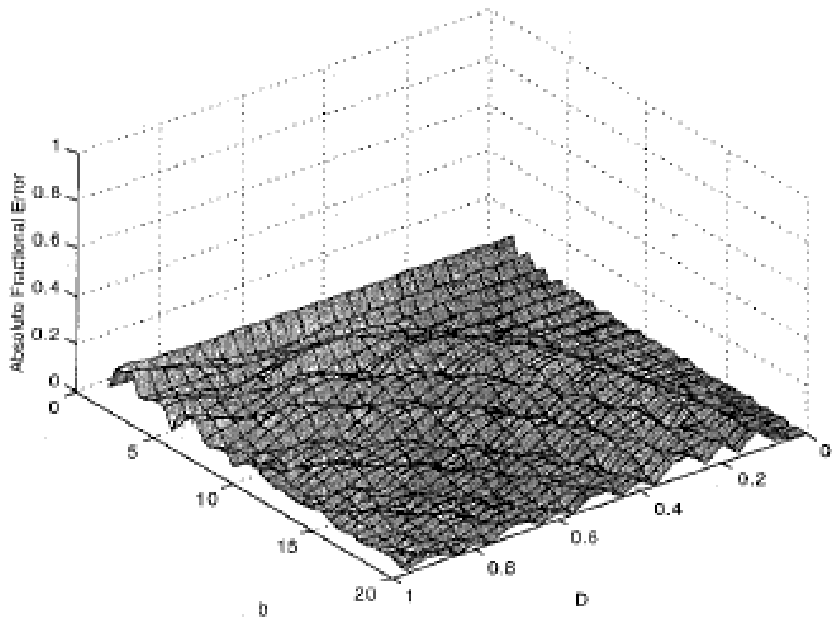

Fig. 11 – Absolute Value of Fractional Error Between New Approximation and Exact Expression

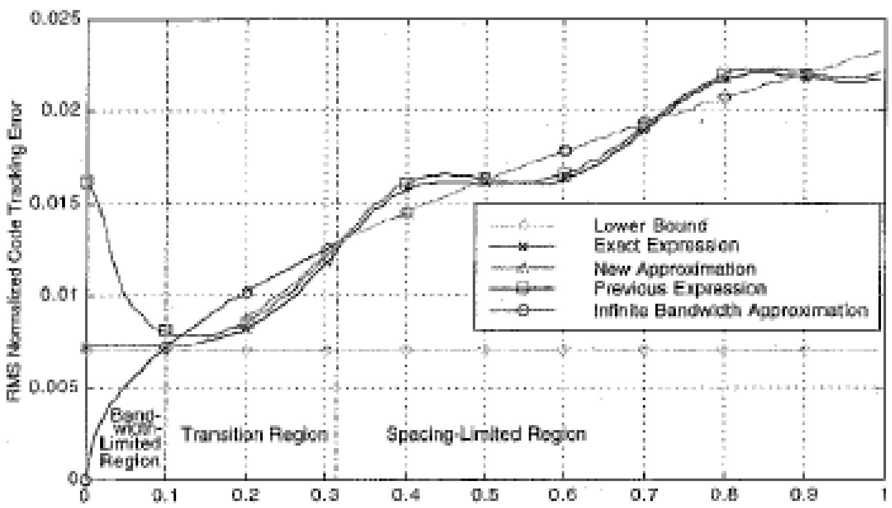

Fig. 12 – Predicted Code-Tracking Error for C_s/N_0 of 30 dB-Hz and Normalized Front-End Bandwidth of 10

nator spacings. However, as the spacing becomes narrower, the infinite bandwidth approximation predicts too large an error, then predicts errors smaller than the LB indicates are achievable. The previous expression matches the exact expression well in the spacing-limited region and the transition region, but has large error in the bandwidth-limited region. In contrast, the new approximation tracks the exact expression much better for the smaller discriminator spacings. Both the exact expression and the new approximation show that with small discriminator spacing, the code-tracking error approaches the lower bound.

Figure 13 shows predicted code-tracking error for the same conditions as Figure 12, except C_s/N_0 of 20 dB-Hz. The results are similar except that with small discriminator spacing, the error approaches an asymptote somewhat greater than the LB. This behavior is due to the squaring loss incurred with noncoherent processing. Since this behavior at lower signal powers is well known, the remaining presentation of results uses the higher C_s/N_0 of 30 dB-Hz.

Figure 14 shows predicted code-tracking error for C_s/N_0 of 30 dB-Hz and normalized front-end bandwidth of b = 3—a moderate front-end bandwidth. The infinite bandwidth approximation exhibits differences from the exact expression for most discriminator spacings, overestimating the error for larger spacings and underestimating it for smaller spacings. The previous expression deviates from the

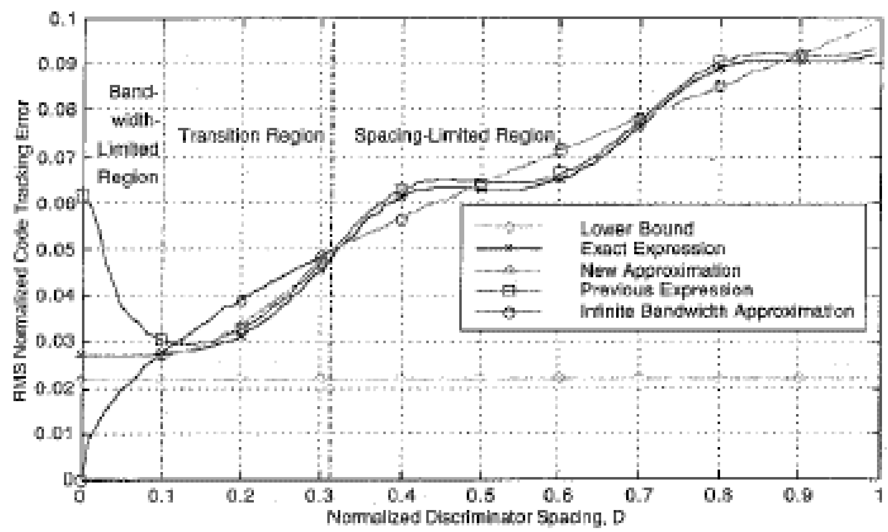

Fig. 13 – Predicted Code-Tracking Error for C_s/N_0 of 20 dB-Hz and Normalized Front-End Bandwidth of 10

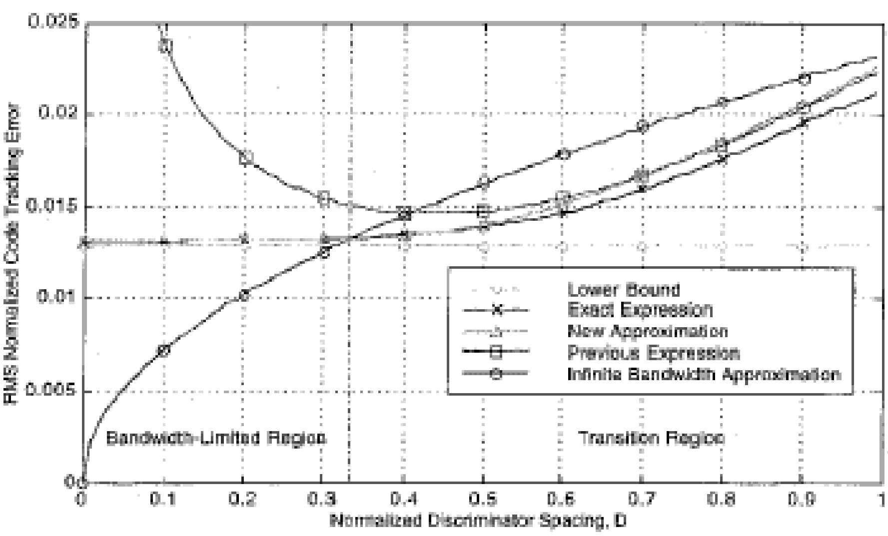

Fig. 14 – Predicted Code-Tracking Error for C_s/N_0 of 30 dB-Hz and Normalized Front-End Bandwidth of 3

exact expression for normalized discriminator spacings less than 0.5, and incorrectly predicts increasing error for smaller spacings. In contrast, the new approximation tracks the exact expression accurately over the range of discriminator spacings.

Figure 15 shows predicted code-tracking error for C_s/N_0 of 30 dB-Hz and normalized front-end bandwidth of b = 1.5—a narrow front-end bandwidth that may be of interest in designing discriminators for the new civil signal at 1176 MHz. While the infinite bandwidth approximation predicts continuing reduced error from smaller discriminator spacings, the previous expression predicts increasing error from smaller discriminator spacings. In contrast, both the new approximation and the exact expression indicate that there is little benefit (in terms of code-tracking accuracy in white noise) to using a discriminator spacing smaller than 1 chip period, but neither does the error increase. This is why the parameter set Db < 1 is called bandwidth-limited: the small bandwidth imposes an inherent limitation on code-tracking accuracy that cannot be overcome with smaller discriminator spacing.

Figure 16 shows predicted code-tracking error for C_s/N_0 of 30 dB-Hz and normalized discriminator spacing of D = 1—a wide spacing. The infinite bandwidth approximation applies well over the wider bandwidths, but does not predict the reduction in code-tracking error obtained at normalized front-end bandwidths near 2. However, the new

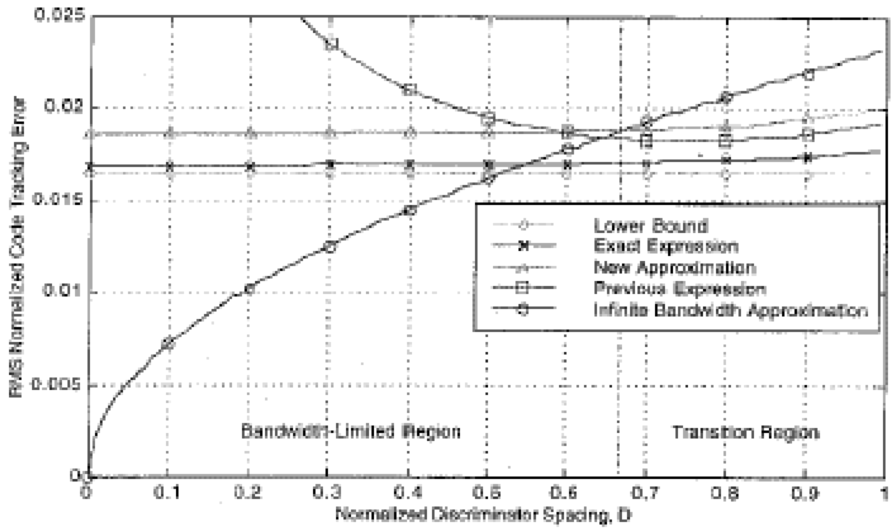

Fig. 15 - Predicted Code-Tracking Error for C_s/N_0 of 30 dB-Hz and Normalized Front-End Bandwidth of 1.5

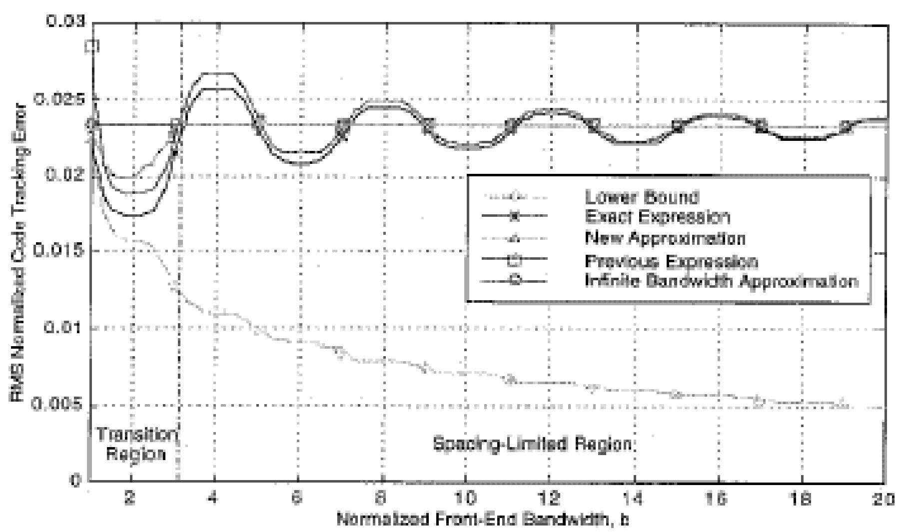

Fig. 16 - Predicted Code-Tracking Error for C_s/N_0 of 30 dB-Hz and Normalized Discriminator Spacing of 1

approximation and previous expression both perform well over the entire range of bandwidths, since the bandwidth-limited region does not occur with wide discriminator spacing. The performance is much worse than the LB, indicating the opportunity to reduce error with smaller discriminator spacing.

Figure 17 shows predicted code-tracking error for C_s/N_0 of 30 dB-Hz and normalized discriminator spacing of D = 0.5—a moderate spacing. The portion of the graph left of the transition region may be of particular interest in designing receivers for the new civil signal at 1176 MHz. The infinite bandwidth approximation applies well over the wider bandwidths, but does not predict the reduction in code-tracking error obtained at normalized front-end bandwidths below 6 or the increase in error for normalized front-end bandwidths smaller than 2. The error predicted by the previous expression is too large for smaller bandwidths. Although the error is smaller than in Figure 16, the performance is still much worse than the LB, indicating the opportunity to reduce error further with even smaller discriminator spacing.

Figure 18 shows predicted code-tracking error for C_s/N_0 of 30 dB-Hz and normalized discriminator spacing of D = 0.1—a narrow spacing. The infinite bandwidth approximation applies well over the wider bandwidths, but does not predict the larger code-tracking error for normalized front-end bandwidths less than 10. In contrast, the previous expression predicts excessively large code-tracking er-

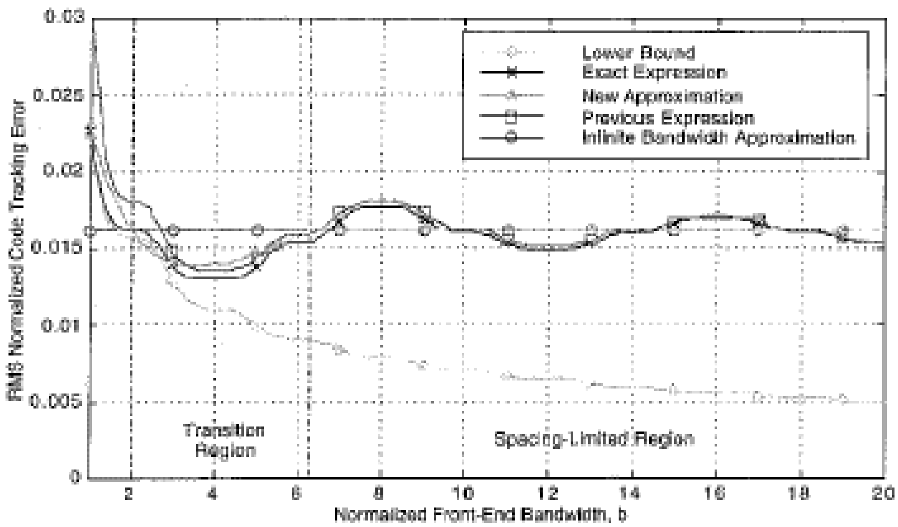

Fig. 17 – Predicted Code-Tracking Error for C_s/N_0 of 30 dB-Hz and Normalized Discriminator Spacing of 0.5

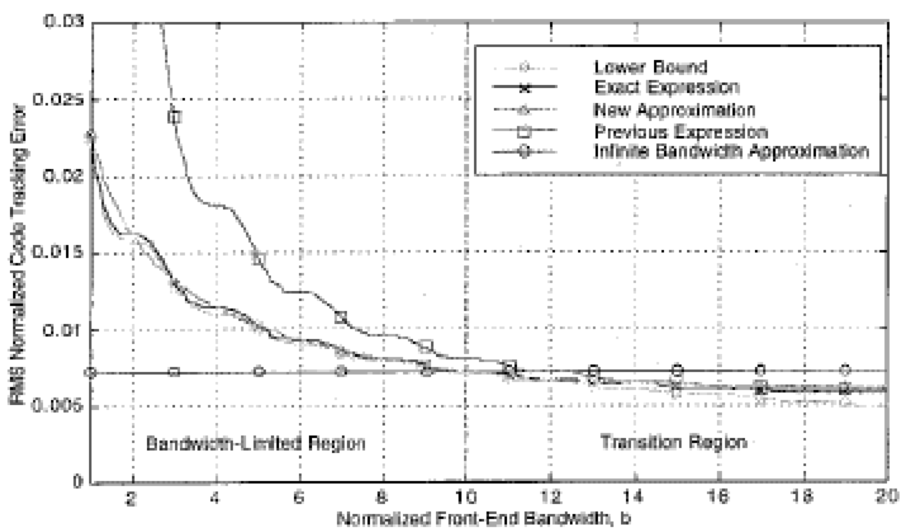

Fig. 18 – Predicted Code-Tracking Error for C_s/N_0 of 30 dB-Hz and Normalized Discriminator Spacing of 0.1

rors for the bandwidth-limited region. Performance is very close to the LB, and is clearly bandwidth-limited for normalized front-end bandwidths less than 10.

The oscillatory behavior of the exact expression for code-tracking error in the spacing-limited region of parameter space can be observed in Figures 10, 11, 14, and 15. In each of these cases, when the receiver design is spacing-limited so that $Db \geq \pi$ there are local minima in code-tracking error for $Db = 2, 6, 10, \ldots$. Conversely, there are local maxima in code-tracking error for $Db = 4, 8, \ldots$. Consequently, there may be advantages in selecting paired values of front-end bandwidth and discriminator spacing that avoid these local maxima and seek the local minima.

CONCLUSIONS

This paper has presented more accurate analytical expressions for the code-tracking accuracy of conventional binary phase shift keyed signals in white noise for limited front-end bandwidth and a code-tracking loop using an early-late discriminator. While evaluation of the exact expressions requires numerical integration, new approximations have been presented that involve only algebraic expressions. An LB on code-tracking error for a bandlimited receiver has also been presented. The new approximation shows that there are three regions of receiver parameter space that must be considered separately. These regions are defined in terms of the normalized front-end bandwidth b, which is the complex bandwidth of the receiver front end multiplied by the signal chip period, and the normalized early-late discriminator spacing D, which is the (two-sided) spacing of the discriminator expressed as a fraction of the signal chip period.

The region defined by $\pi \leq Db$ is referred to as *spacing-limited*, since the error depends primarily on the early-late spacing and not the front-end bandwidth. The infinite bandwidth approximation [1] applies for this set of receiver parameters, but does not apply for other parameter values. The region defined by $Db < 1$ is referred to as *bandwidth-limited*, since the error depends primarily on the front-end bandwidth and not the early-late spacing. The condition $1 < Db < \pi$ indicates a transition region between the two distinct limiting cases. The previous expression for the bandlimited case is incorrect for the bandwidth-limited case since it does not account for the effect of bandlimiting on the noise correlation—an important effect for narrow discriminator spacings.

The new approximations presented in this paper are accurate over the range of front-end bandwidths and discriminator spacings, and can be evaluated readily since they involve only algebraic expressions. The results show that there is no performance penalty (in the sense of increased code-tracking error) for very small discriminator spacings. Recent work [10] has also verified the purely theoretical results in this paper with experimental results.

Discriminator performance using parameter values associated with the bandwidth-limited and transition regions is likely to take on increasing importance with the higher chip rate signals proposed for the new civil signal on L5, and with continuing interest in narrow correlator spacing for multipath processing as well as improved code-tracking accuracy. Either the exact expression or the new approximation presented in this paper should be employed.

ACKNOWLEDGMENTS

This work was sponsored by the U.S. Air Force under contract number F19628-99-C-0001. The authors express their appreciation to Dr. Christopher Hegarty for his suggestions on the presentation of this work.

APPENDIX

GENERAL EXPRESSIONS FOR CODE-TRACKING ERROR IN GAUSSIAN NON-WHITE NOISE PLUS INTERFERENCE

This appendix presents general analytical results for code-tracking accuracy, as derived in [4, 5]. Special cases of these expressions for bandlimited white noise and conventional binary phase shift keyed signals have been developed in the main body of this paper.

When the integration time used to form a correlation estimate in the discriminator is T seconds (assumed to be much longer than the signal's spreading code period), the bandlimiting at the receiver is represented by a rectangular bandpass filter with complex bandwidth β_r Hz (assumed to be much larger than $1/T$); B_L is the one-sided code-tracking loop bandwidth, in hertz (assumed to be less than $0.5/T$); Δ is the (two-sided) early-late spacing in seconds; $G_s(f)$ is the normalized (unit area) power spectral density of the signal in 1/hertz, assumed to be symmetric; C_s is the signal carrier power over infinite bandwidth in watts; $G_w(f)$ is the power spectral density of Gaussian noise plus interference in watts/hertz; and a code-tracking loop using noncoherent early-late processing (NELP) has output variance, in units of seconds squared, of

$$(\sigma_\tau^2)_{NELP} = B_L(1 - 0.5B_LT)\left[\frac{\int_{-\beta_r/2}^{\beta_r/2} G_w(f)G_s(f)\sin^2(\pi f\Delta)\,df}{(2\pi)^2C_s\left(\int_{-\beta_r/2}^{\beta_r/2} fG_s(f)\sin(\pi f\Delta)\,df\right)^2} + \frac{\left(\int_{-\beta_r/2}^{\beta_r/2} G_w(f)G_s(f)\,df\right)^2 - \left|\int_{-\beta_r/2}^{\beta_r/2} G_w(f)G_s(f)e^{i2\pi f\Delta}\,df\right|^2}{4(2\pi)^2TC_s^2\left(\int_{-\beta_r/2}^{\beta_r/2} fG_s(f)\sin(\pi f\Delta)\,df\int_{-\beta_r/2}^{\beta_r/2} G_s(f)\cos(\pi f\Delta)\,df\right)^2}\right] \quad (12)$$

In contrast, a code-tracking loop using coherent early-late processing (CELP) has output variance, also in units of seconds squared, of

$$(\sigma_\tau^2)_{CELP} = B_L(1 - 0.5B_LT) \times \left[\frac{\int_{-\beta_r/2}^{\beta_r/2} G_w(f)G_s(f)\sin^2(\pi f\Delta)\,df}{(2\pi)^2C_s\left(\int_{-\beta_r/2}^{\beta_r/2} fG_s(f)\sin(\pi f\Delta)\,df\right)^2}\right] \quad (13)$$

A lower bound (LB) on code-tracking loop output variance is obtained by computing the Cramér-Rao lower bound on time-of-arrival estimation for integration time T, then assuming the estimates are smoothed with the code-tracking loop, yielding the LB

$$(\sigma_\tau^2)_{LB} = B_L(1 - 0.5B_LT) \times \left[\frac{1}{(2\pi)^2C_s\int_{-\beta_r/2}^{\beta_r/2} f^2\frac{G_s(f)}{G_w(f)}\,df}\right] \quad (14)$$

REFERENCES

1. Van Dierendonck, A. J., P. Fenton, and T. Ford, *Theory and Performance of Narrow Correlator Spacing in a GPS Receiver*, NAVIGATION, Journal of The Institute of Navigation, Vol. 38, No. 3, Fall 1992, pp. 265–283.
2. Holmes, J. K., *Noncoherent Late Minus Early Power Code Tracking Loop Performance with Front End Filtering*, Proceedings of ION GPS-97, The Institute of Navigation, September 1997.
3. Spilker, J. J., *Proposed New Civil GPS Signal at 1176.45 MHz*, Proceedings of ION GPS-99, The Institute of Navigation, September 1999.
4. Kolodziejski, K. R. and J. W. Betz, *Effect of Non-White Gaussian Interference on GPS Code-Tracking Accuracy*, Technical Report MTR99B21R1, The MITRE Corporation, McLean, VA, June 1999.
5. Betz, J. W., and K. R. Kolodziejski, *Generalized Theory of GPS Code-Tracking Accuracy with an Early-Late Discriminator*, Submitted to IEEE Transactions on Aerospace and Electronic Systems, July 2000.
6. Parkinson, B. W. and J. J. Spilker, Jr. (eds.), *Global Positioning System: Theory and Applications, Volume I*, Progress in Astronautics and Aeronautics, Volume 163, 1996.
7. Betz, J. W., *The Offset Carrier Modulation for GPS Modernization*, Proceedings of The Institute of Navigation's 1999 National Technical Meeting, January 1999.
8. Betz, J. W., *Effect of Narrowband Interference on GPS Code-Tracking Accuracy*, Proceedings of ION-2000, The Institute of Navigation, January 2000.
9. Holmes, J. K., *Coherent Spread Spectrum Systems*, Krieger Publishing, 1990.
10. Stephens, S. A. and J. B. Thomas, *Controlled-Root Formulation for Digital Phase-Locked Loops*, IEEE Transactions on Aerospace and Electronic Systems, Vol. 31, No. 1, January 1995, pp. 78–95.
11. Betz, J. W., *Effect of Narrow Correlator Spacing on Code-Tracking Accuracy*, Proceedings of The Institute of Navigation's 1999 National Technical Meeting, January 2000.